

NMR of Biopolymer-Apatite Composites: Developing a Model of the Molecular Structure of the Mineral-Matrix Interface in Calcium Phosphate Biomaterials

Joanna V. Bradley,[†] Lydia N. Bridgland,[†] Dawn E. Colyer,[†] Melinda J. Duer,^{*,†} Tomislav Friščić,[†] James R. Gallagher,[†] David G. Reid,[†] Jeremy N. Skepper,[‡] and Christine M. Trasler[†]

[†]Department of Chemistry University of Cambridge Lensfield Road Cambridge CB2 1EW United Kingdom, and [‡]Department of Physiology, Development & Neuroscience University of Cambridge Downing Street Cambridge CB2 3DY United Kingdom

Received June 21, 2010. Revised Manuscript Received September 17, 2010

Nanoparticulate hydroxyapatites (HAPs) reproducing some of the subnanometre length scale intermolecular interactions characteristic of hard tissue have been prepared for nuclear magnetic resonance (NMR) structural elucidation. HAPs were precipitated at physiological pH and temperature from dilute aqueous solutions, in the presence of acidic polysaccharides (chondroitin sulfate, dermatan sulfate, hyaluronic acid, dextran sulfate, polygalacturonic acid), and of hydrophilic poly aminoacids (poly-L-glutamate, poly-L-asparagine, poly-L-lysine). The HAP resembles that of bone with respect to its ³¹P NMR properties, broad reflections in X-ray powder diffraction, and the coexistence of an ordered crystalline core, surrounded by a less ordered surface containing water and hydrogen phosphate. ¹³C{³¹P} rotational echo double resonance (REDOR) NMR, which probes carbon–phosphorus proximities below ca. 1 nm, shows that all the HAPs are molecular composites in which each biopolymer forms intimate intermolecular associations with mineral ions. REDOR effects between mineral phosphorus and ring carbons of the polysaccharides, and the side-chain terminal carboxylate and amide carbonyls of poly-L-glutamate and poly-L-asparagine, and the side chain carbons of poly-L-lysine, closely recapitulate those seen in native bone. Such model HAP–biopolymer composites will prove useful in studies of the role of biopolymers in biomineralization, and in high resolution biomineral structure elucidation.

Introduction

Naturally occurring biominerals are generally complex composites between inorganic salts and biopolymers and other organic species.^{1–3} This is true both of biomineral elaborated under conditions of healthy growth, such as normal bone, dentine, and mineralizing cartilage, and that which can evolve in disease states, including calcified atherosclerotic plaque,⁴ and certain types of urinary calculi.⁵ Whether and if so how the underlying biopolymers control mineralization is a matter of considerable

debate and importance.⁶ Whatever these mechanisms are they will be central in understanding and controlling pathological mineralization and repairing damaged native mineralized tissues. They are also crucial in ensuring the faithful integration with host tissue of artificial surgically implantable materials. This work seeks to elucidate the role played by a broad spectrum of biopolymers by examining in detail the nature of the mineral produced in the presence of each and how it interacts (if at all) with the biopolymer, as the manner of interaction in the final material gives useful information about the mechanism of formation.

Numerous theories have been advanced about how biomineralization is initiated and controlled.^{7,8} Many invoke templating and control based on the recognition of Ca²⁺ by a variety of biomolecules, such as acidic proteins rich in aspartate, glutamate and its derivative γ -carboxyglutamate, phosphorylated residues such as phosphoserine,⁹ and also acidic glycosaminoglycans

*Corresponding author. Phone: (+44)(0)763934. Fax: (+44)(0)336362. E-mail: mjd13@cam.ac.uk.

- (1) *Principles of Bone Biology*; Bilezikian, J. P., Raisz, L. G., Rodan, G. A., Ed.; Academic Press: New York, 2002.
- (2) Veis, A., Mineralization in organic matrix frameworks. In *Biomineralization*; Patricia, M. Dove, J. J. D. Y., Steve Weiner, Ed.; The Mineralogical Society of America: Washington DC, 2003; Vol. 54, pp 249.
- (3) Vincent, J., *Structural Biomaterials*; Princeton University Press: Princeton, NJ, 1990.
- (4) Duer, M. J.; Frisic, T.; Proudfoot, D.; Reid, D. G.; Schoppet, M.; Shanahan, C. M.; Skepper, J. N.; Wise, E. R. *Arterioscler., Thromb. Vasc. Biol.* **2008**, 28, 2030.
- (5) Pramanik, R.; Asplin, J. R.; Jackson, M. E.; Williams, J. C., Jr. *Urol. Res.* **2008**, 36, 251.
- (6) Gokhale, J. A.; Boskey, A. L.; Robey, P. G., The biochemistry of bone. In *Osteoporosis*; Marcus, R.; Feldman, D.; Kelsey, J., Eds.; Academic Press: New York, 2001; Vol. 1, p 107.

(7) Currey, J. D., *Bones: Structure and Mechanics*; Princeton University Press: Princeton, 2002.

(8) Mann, S., Biomineralization: principles and concepts in bioinorganic materials chemistry. In *Oxford Chemistry Masters*; Richard, G. Compton, S. G. D., John Evans, Ed.; Oxford University Press: Oxford, 2001; p 198.

(GAGs) and other polysaccharides, which are significant bone constituents.¹⁰ It has been postulated many times that the biopolymer provides a base for the initial organization of mineral ions into a crystallographic layer. Biomolecules are also presumed to play an inhibitory role in mineralization by binding to specific crystal surfaces thus preventing further growth of that surface.¹¹ Studies of small proteins like the salivary peptide statherin^{12–15} and the dental enamel amelogenin,^{16,17} and fragments thereof, binding to hydroxyapatite have shown conclusively that such binding of proteins occurs and via specific amino acid residues.

Biomimetic Structure and NMR (Nuclear Magnetic Resonance). Mineralization in vertebrates typically involves the precipitation of calcium phosphate to a mineral phase resembling nanoparticulate HAp and occurs within a scaffold of collagen fibrils containing numerous other proteins and GAGs. The apatite mineral tolerates diverse substitutions from its idealized formulation as $\text{Ca}_{10}(\text{PO}_4)_6(\text{OH})_2$, typically of carbonate¹⁸ and other anions for hydroxyl and phosphate, and of sodium or magnesium for calcium.¹⁹

NMR spectroscopy is particularly effective at studying such complex materials. As far as biomimetic apatite particles are concerned NMR reveals grading from a highly crystalline interior to a disordered hydrated surface with abundant hydrogen phosphate substitutions.^{20–22} Moreover the predominance of ^{31}P and ^{13}C in the mineral and organic phases respectively is very fortunate. This is because it enables the structure of the mineral–organic interface to be effectively studied using double resonance NMR experiments of which $^{13}\text{C}\{^{31}\text{P}\}$ rotational echo double resonance (REDOR)^{23–25} is particularly valuable.²⁶ However, while REDOR reveals marked and

consistent similarities of the interface in a variety of mineralized materials^{4,27–29} lack of spectral resolution in the native materials prevents the assignment of specific REDOR effects to specific molecules. For instance while REDOR might implicate GAGs in interfacial binding it is not possible to ascribe this participation to a definite class of GAG molecule. Similarly numerous REDOR effects are observed to protein signals which at best can be assigned only to amino acid residue type (e.g., proline, hydroxyproline) and functionality (e.g., carboxylate, carbonyl, methyl, etc.) including tentatively to γ -carboxylglutamate.²⁷

In this work, we form biomimetic HAp particles under conditions resembling biological with respect to temperature and pH, and at millimolar reagent concentrations, in the presence of a wide range of biopolymers. We employ solid-state NMR spectroscopy supported by X-ray powder diffraction (XRD) and scanning electron microscopy (SEM) to examine how the nature of the biopolymer affects the resulting mineral structure, including the surface structures of the particles. At the same time the simplicity of the ^{13}C NMR spectrum of the HAp–biopolymer composite facilitates a more detailed interpretation of REDOR effects in terms of interactions between specific biopolymer functional groups and mineral phosphate groups. We have chosen a wide variety of biopolymers–GAGs important in mammalian connective tissues, other anionic polysaccharides, and anionic, uncharged polar, and cationic polypeptides. We find the structure of the mineral formed, in respect of hydration, hydrogen phosphate substitutions, crystallinity, and particle size does not depend on the biopolymer, and yet all biopolymers employed show close contact with the mineral as judged by REDOR NMR experiments. Although the syntheses were performed at supersaturated reagent concentrations, a possible interpretation of this lack of specificity is that the biopolymers are not templating a particular crystallographic structure but provide a collection mechanism for the constituent ions. Additionally it seems that the HAp nanoparticle structure, or part of it, is able to accommodate essentially unperturbed a range of biopolymer motifs.

Materials and Methods

Preparation of HAp–Biopolymer Composites. The following biopolymers (as the sodium salts unless stated otherwise) were purchased from Sigma Chemical Co. (Poole, Dorset, United Kingdom) and were used without further preparation: Chondroitin sulfate from bovine trachea (a mixture containing ca. 70% of the galactosamine-4-sulfate and 30% of the galactosamine-6-sulfate forms); dermatan sulfate as the potassium salt from porcine intestinal mucosa; hyaluronic acid as the potassium salt from human umbilical cord; polygalacturonic acid (pectin) from citrus fruit; dextran sulfate (average molecular

- (9) Wu, Y.; Ackerman, J. L.; Strawich, E. S.; Rey, C.; Kim, H. M.; Glimcher, M. J. *Calcif. Tissue Int.* **2003**, *72*, 610.
- (10) Robey, P. G.; Bone matrix proteoglycans and glycoproteins. In *Principles of Bone Biology*, 2nd ed.; Bilezikian, J. P., Raisz, L. G., Rodan, G. A., Eds.; Academic Press: New York, 2002; Vol. 1, pp 225.
- (11) Shaw, W. J.; Ferris, K. J. *J. Phys. Chem. B* **2008**, *112*, 16975.
- (12) Gibson, J. M.; Popham, J. M.; Raghunathan, V.; Stayton, P. S.; Drobny, G. P. *J. Am. Chem. Soc.* **2006**, *128*, 5364.
- (13) Ndao, M.; Ash, J. T.; Breen, N. F.; Goobes, G.; Stayton, P. S.; Drobny, G. P. *Langmuir* **2009**, *25*, 12136.
- (14) Goobes, G.; Goobes, R.; Shaw, W. J.; Gibson, J. M.; Long, J. R.; Raghunathan, V.; Schueler-Furman, O.; Popham, J. M.; Baker, D.; Campbell, C. T.; Stayton, P. S.; Drobny, G. P. *Magn. Reson. Chem.* **2008**, *45*, S32.
- (15) Long, J. R.; Shaw, W. J.; Stayton, P. S.; Drobny, G. P. *Biochemistry* **2001**, *40*, 15451.
- (16) Shaw, W. J.; Campbell, A. A.; Paine, M. L.; Snead, M. L. *J. Biol. Chem.* **2004**, *279*, 40263.
- (17) Shaw, W. J.; Ferris, K.; Tarasevich, B.; Larson, J. L. *Biophys. J.* **2008**, *94*, 3247.
- (18) Fleet, M. E.; Liu, X. *Biomater.* **2005**, *26*, 7548.
- (19) Elliott, J. C. *Structure and Chemistry of the Apatites and Other Calcium Orthophosphates*; Elsevier: New York, 1994.
- (20) Cho, G.; Wu, Y.; Ackerman, J. L. *Science* **2003**, *300*, 1123.
- (21) Maltsev, S.; Duer, M. J.; Murray, R. C.; Jaeger, C. J. *Mater. Sci.* **2007**, *42*, 8804.
- (22) Tseng, Y. H.; Mou, Y.; Chen, P. H.; Tsai, T. W.; Hsieh, C. I.; Mou, C. Y.; Chan, J. C. *Magn. Reson. Chem.* **2008**, *46*, 330.
- (23) Gibson, J. M.; Raghunathan, V.; Popham, J. M.; Stayton, P. S.; Drobny, G. P. *J. Am. Chem. Soc.* **2005**, *127*, 9350.
- (24) Mueller, K. T. *J. Magn. Reson. Series A* **1995**, *113*, 81.
- (25) Pan, Y.; Gullion, T.; Schaeffer, J. J. *Magn. Reson.* **1990**, *90*, 330.
- (26) Jaeger, C.; Groom, N. S.; Bowe, E. A.; Horner, A.; Davies, M. E.; Murray, R. C.; Duer, M. J. *Chem. Mater.* **2005**, *17*, 3059.

- (27) Duer, M. J.; Friscic, T.; Murray, R. C.; Reid, D. G.; Wise, E. R. *Biophys. J.* **2009**, *96*, 3372.
- (28) Reid, D. G.; Duer, M. J.; Murray, R. C.; Wise, E. R. *Chem. Mater.* **2008**, *20*, 3549.
- (29) Wise, E. R.; Maltsev, S.; Davies, M. E.; Duer, M. J.; Jaeger, C.; Loveridge, N.; Murray, R. C.; Reid, D. G. *Chem. Mater.* **2007**, *19*, 5055.

weight ca. 8,000) from *Leuconostoc* species; poly-L-glutamate (average molecular weight 1500–5000); poly-L-asparagine (average molecular weight 5000–15 000); poly-L-lysine as the bromide (average molecular weight 4000–15 000). Nanocrystalline hydroxyapatite (HAp) and HAp–biopolymer composites were prepared by modification of literature methods³⁰ to more closely reflect biological conditions (avoiding extremes of pH, temperature, and ammonium ion concentration) as follows: Calcium chloride hexahydrate (7.8 mmol) and dipotassium hydrogen phosphate (4.7 mmol) were separately dissolved in ca. 500 mL distilled water. For the HAp–biopolymer composites, about 120 mg of each biopolymer was also dissolved into the potassium phosphate solution. The calcium chloride solution was then added to the stirred potassium phosphate solution over one hour using a peristaltic pump, whereas the pH of the reaction mixture was maintained at 7.4 by addition of dilute sodium hydroxide solution. The resultant slurry was aged for 24 h then filtered, washed with distilled water, and air-dried. Weight percent of organic material incorporated into each composite was determined by conventional C, H, and N microanalysis.

Solid State NMR Measurements. All experiments were performed on a Bruker 400 MHz Avance spectrometer equipped with a standard triple resonance solid state probe, at frequencies of 400.1 MHz (¹H), 161.9 MHz (³¹P) and 100.5 MHz (¹³C), at a magic angle spinning (MAS) rate of 12.5 kHz, with samples packed into 4 mm zirconia rotors (Bruker). All samples were first characterized using standard cross-polarization (CP) MAS techniques (¹H $\pi/2$ pulse length 2.5 μ s, ¹H cross-polarization field 70 kHz, ¹H–³¹P cross-polarization contact time 10 ms, ¹H–¹³C cross-polarization contact time 2.5 ms, broadband TPPM15 decoupling during signal acquisition at a ¹H field strength of 100 kHz). ¹H–³¹P heteronuclear correlation (HETCOR) experiments were performed using Lee–Goldburg cross-polarization from ¹H to ³¹P for times which varied between 2 and 8 ms. Chemical shifts were referenced to 85% phosphoric acid at 0 ppm (³¹P), and the methylene signal from glycine at 43.1 ppm relative to tetramethylsilane at 0 ppm (¹³C). ¹³C{³¹P} REDOR measurements were performed³¹ by applying a series of ³¹P π pulses (8 μ s) synchronized with the rotation period (80 μ s) of the MAS subsequent to ¹H–¹³C cross-polarization, with a ¹³C refocusing π pulse (8 μ s) at the midpoint of the ³¹P pulse train. The number of rotor cycles in the REDOR sequence was either 60 or 120, producing dephasing times of 4.8 or 9.6 ms, respectively. ¹H dipolar dephasing experiments were performed at an MAS frequency of 6.25 kHz using a rotor synchronized spin echo, ¹³C π refocusing pulse of 6 μ s and 160 μ s for each half echo. The dipolar dephasing period during which broad band ¹H decoupling is not implemented was inserted during the initial part of the first half of the spin echo. Repetition time was 2 s in all experiments.

X-ray Diffraction (XRD). XRD was performed on the composite powders using a Philips X'Pert Pro powder diffractometer equipped with an X'celerator RTMS detector, using Ni-filtered CuK α radiation. Data collection was performed in a 5–80° range using samples on a flat glass plate, with a scanning step size of 0.008°, time per step of 10.8 s and scan speed of 0.0985 °/s.

Scanning Electron Microscopy (SEM). Synthetic HAp and HAp–biopolymer composite mineral particles were dusted onto

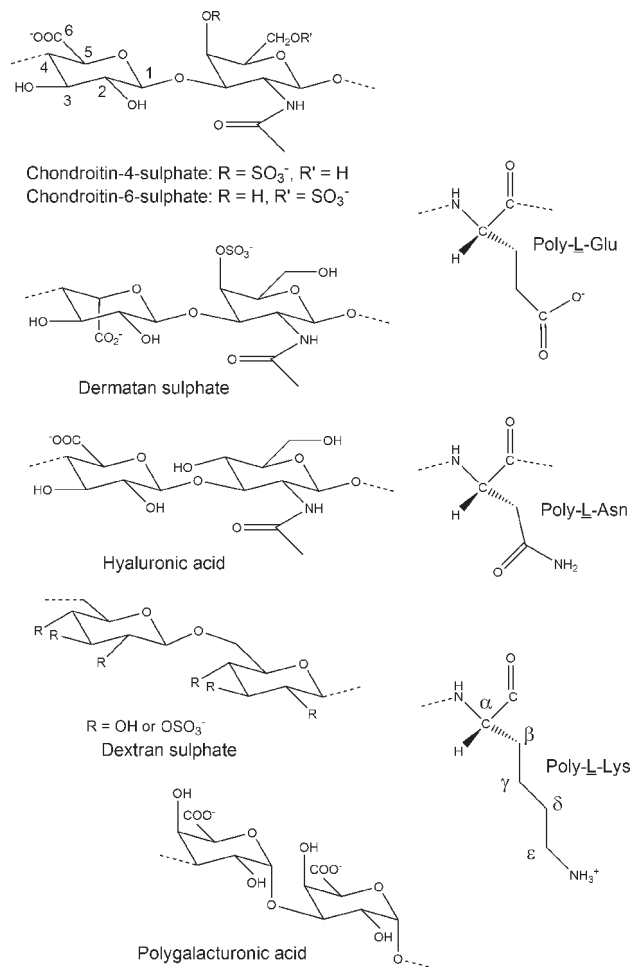


Figure 1. Chemical structural formulas of the repeat unit of each of the biopolymers studied. The numbering/naming conventions for sugar rings and amino acid residues are exemplified in the chondroitin sulfate and poly-L-lysine structures, respectively.

spectroscopically pure double sided carbon tabs mounted on Cambridge SEM stubs and viewed in a FEI Phillips XL30 FEGSEM operated at 5 kV.

Results

Characterization of the Synthetic HAp–Biopolymer Composites. Chemical structural formulas of the biopolymers used are shown in Figure 1. Production of nanocrystalline HAp by the methods described above was initially checked for all materials by the observation of a broad (half height line width ca. 650 Hz, ca. 4 ppm) ³¹P NMR signal at a chemical shift (i.e., resonance frequency) of ca. 2.5 ppm, accompanied by weak spinning side bands.³² Definitive proof of the formation of HAp came from by XRD; Figure 2 compares the XRD properties of native bone, our synthetic HAp, and commercial macrocrystalline HAp. The first two materials are remarkably similar to each other, and display all the reflections of the macrocrystalline material, only broadened by structural disorder, the nanocrystalline nature of the mineral particles, or a combination of both factors.

(30) Welzel, T.; Meyer-Zaika, W.; Eppe, M. *Chem. Commun.* **2004**, 1204.

(31) Duer, M. J., *Introduction to Solid-State NMR Spectroscopy*; Blackwell Science: Oxford, 2004; p 116.

(32) Belton, P. S.; Harris, R. K.; Wilkes, P. J. *J. Phys. Chem. Solids.* **1988**, *49*, p 21.

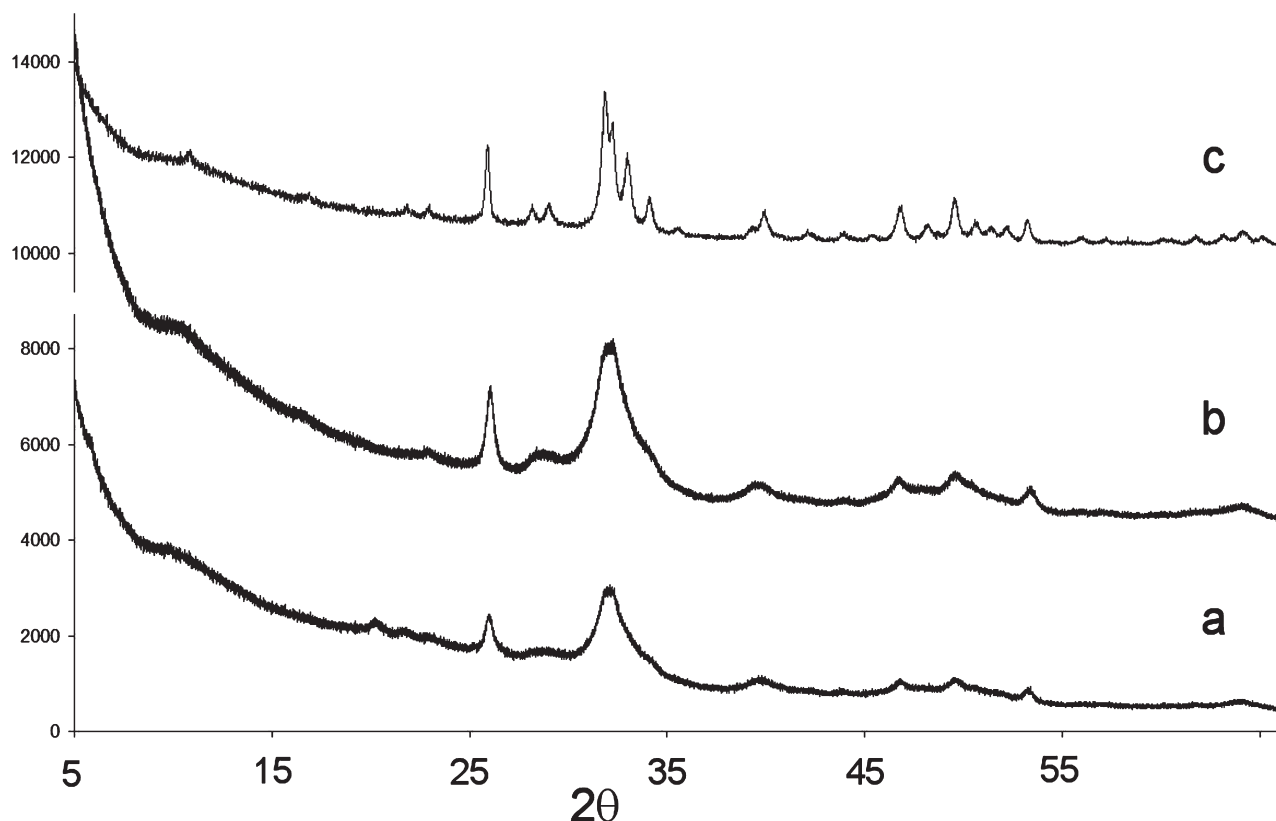


Figure 2. XRD traces of (a) native bone, (b) synthetic HAp prepared as described, and (c) commercial macrocrystalline HAp.

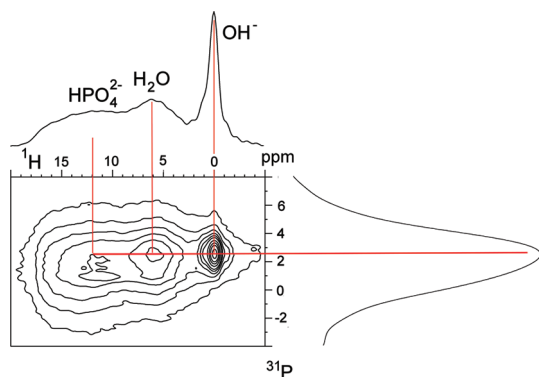


Figure 3. Typical ^1H – ^{31}P HETCOR data, acquired on HAp composited with bovine tracheal chondroitin sulfate using ^1H – ^{31}P Lee–Goldburg cross-polarization of 8 ms duration. The rectangular panel is a two-dimensional contour plot of spectral intensity. It maps the chemical shifts of ^1H atoms (horizontal axis) to the chemical shifts of ^{31}P atoms (the vertical axis) to which they are close in space (within less than 1 nm). The horizontal red line connects chemical shifts of hydrogens which are close to HAp phosphorus atoms distinguished by a ^{31}P chemical shift of 2.5 ppm. The trace above the contour plot is a slice extracted along this ^{31}P chemical shift axis; the trace to the right of the contour plot is a ^{31}P spectrum rotated through 90° to correspond to the vertical orientation of the ^{31}P chemical shift axis. The axes are oriented in this way so that the ^1H slice assumes the horizontal orientation with which chemists are most familiar, with ^1H chemical shift frequency increasing from right to left.

More detailed investigations on key samples used the ^1H – ^{31}P heteronuclear correlation (HETCOR) experiment; typical results are shown in Figure 3. The significance of the experiment is best appreciated by extracting a horizontal cross section at a ^{31}P frequency of 2.5 ppm, and this extracted cross section is shown in the upper panel. It is effectively a ^1H spectrum of the HAp component of the composite and is a

distinctive hallmark of biogenic apatites.^{20,27} Signals at ^1H chemical shifts of ca. 0 ppm, 6 ppm, and 12 ppm are assigned, respectively, to OH^- , H_2O , and HPO_4^{2-} species, respectively, included in the HAp lattice or its more disordered and hydrated surface. The synthesized HAp contains a small fraction of a poorly structured phosphate giving rise to a weak broad shoulder at a ^{31}P chemical shift of ca. –5 ppm on the main HAp signal. It shows some correlations to water and hydrogen phosphate protons.

The nanoparticulate nature of the HAp composites was confirmed by scanning electron microscopy (SEM), and Figure 4 shows typical micrographs. All mineral particles examined were aggregates of smaller particles of typical dimensions of a few tens of nanometers.

Successful coprecipitation of significant quantities of each biopolymer with the HAp was confirmed by conventional organic chemical microanalysis (Table 1), and by the observation of ^{13}C CP-MAS spectra consistent with the biopolymer chemical structure.

NMR of the Mineral–Biopolymer Interface. The $^{13}\text{C}\{^{31}\text{P}\}$ REDOR procedure for each of the five HAp:polysaccharide composites produced significant dephasing of spectral intensity and typical data are shown in Figure 5. Each experiment consists of two outputs; a reference spectrum (black) with no REDOR effect, overlain by a spectrum showing REDOR (red). In general the REDOR responses of the biopolymers to compositing with HAp are similar to those already reported for HAp composited with shark cartilage chondroitin sulfate (*N*-acetylgalactosamine-4-sulfate: *N*-acetylgalactosamine-6-sulfate ca. 90:10).³³

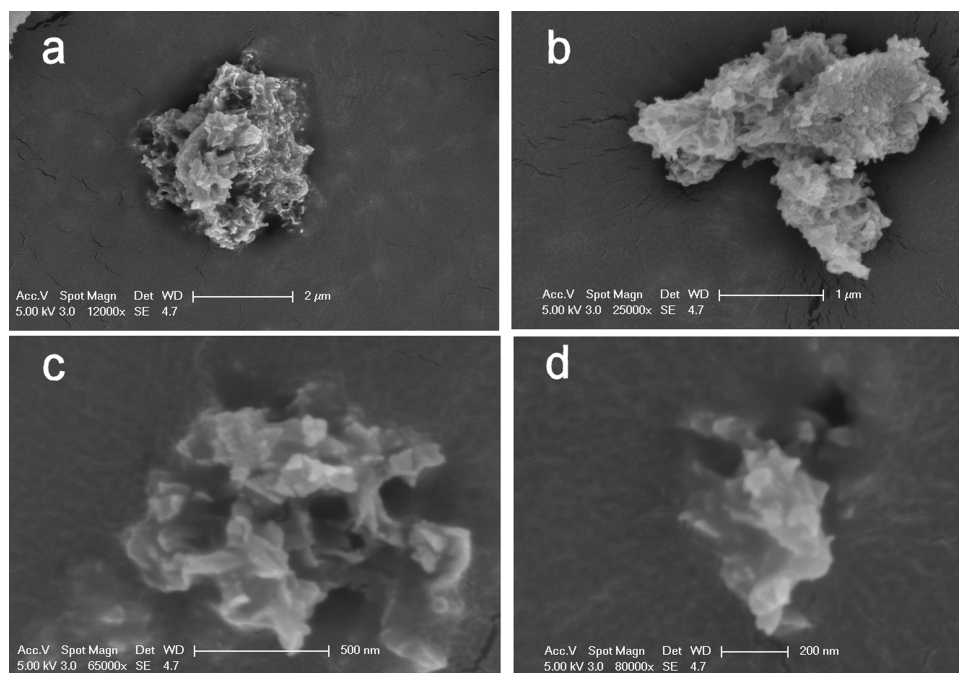


Figure 4. Typical scanning electron micrographs of synthetic HAp, at magnification factors of 12 000 (a), 25 000 (b), 65 000 (c), and 80 000 (d). The data shown was obtained on pure HAp; this and all the composite materials are aggregates of particles of several tens of nanometers in size.

Table 1. Conventional Elemental Microanalysis Data for the Pure Composites^a

| HAp-biopolymer composite | weight % | | |
|--------------------------|-------------------|----------|----------|
| | carbon | hydrogen | nitrogen |
| pure HAp | 0.25 ^b | 1.15 | 0.0 |
| chondroitin sulfate | 4.53 | 1.78 | 0.8 |
| dermatan sulfate | 3.04 | 2.30 | 0.30 |
| hyaluronic acid | 2.42 | 2.11 | 0.27 |
| dextran sulfate | 1.57 | 1.91 | 0.00 |
| polygalacturonic acid | 3.41 | 2.83 | 0.00 |
| polyGlu | 4.65 | 2.08 | 1.08 |
| polyAsn | 4.02 | 2.20 | 2.08 |
| polyLys | 4.49 | 2.32 | 1.85 |

^a All determinations were performed in duplicate. In no case did the measured elemental weight percent of either determination differ by more than 0.1%. ^b Ascibed to inorganic carbonate ion.

REDOR data for HAp composited with the three poly amino acids are shown in Figure 6. Again the effects are reminiscent of those reported for a HAp-poly-L-aspartate composite.³³

The fractional REDOR effects at 9.6 ms dephasing time for each resolved signal of each of the composites are shown in Table 2. Time dependences of the REDOR effects (4.8 and 9.6 ms dephasing times) are available as Supporting Information. Interestingly the comparable strength of the REDOR effects across the three poly amino acid materials, one constituted from a polyanion, another from a neutral polar species, the third from a polycation, illustrates the versatility of HAp as a partner in such composites. Also shown is a control experiment performed on a simple mixture prepared by grinding poly-L-lysine with pure HAp; no REDOR effects are

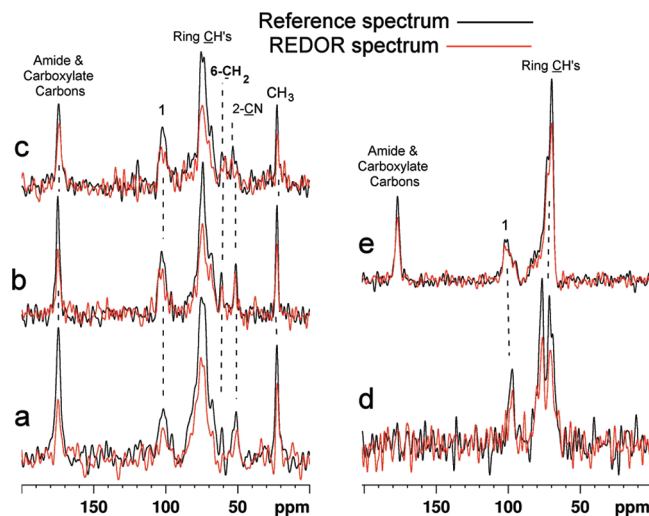


Figure 5. Typical $^{13}\text{C}\{^{31}\text{P}\}$ REDOR data from HAp composited with bovine tracheal chondroitin sulfate (a), dermatan sulfate (b), hyaluronic acid (c), dextran sulfate (d), and polygalacturonic acid (e). Each black trace is a reference ^{13}C spectrum acquired without the $^{31}\text{P} - ^{13}\text{C}$ through-space magnetic dipole–dipole coupling, while each red trace was acquired under identical conditions to the black trace it overlays, except that the phosphorus–carbon magnetic dipole–dipole interaction was activated by the REDOR procedure (for 9.6 ms in each case shown). Signals from structurally different carbon atoms lose intensity during the REDOR period, to a greater or lesser extent depending on whether they are close to or distant from neighboring phosphorus atoms respectively. This signal loss is often referred to as “dephasing”. Chemically analogous carbon signals in different compounds are connected by vertical dashed lines.

observed, consistent with the coexistence of discrete particles of each substance, and proving that a positive REDOR result is a sensitive proof of the formation of an intermolecular composite.

In native bone, although the strongest REDOR effects are seen to a signal at ca. 76 ppm, which chemical shift

(33) Best, S. M.; Duer, M. J.; Reid, D. G.; Wise, E. R.; Zou, S. *Magn. Reson. Chem.* **2008**, *46*, 323.

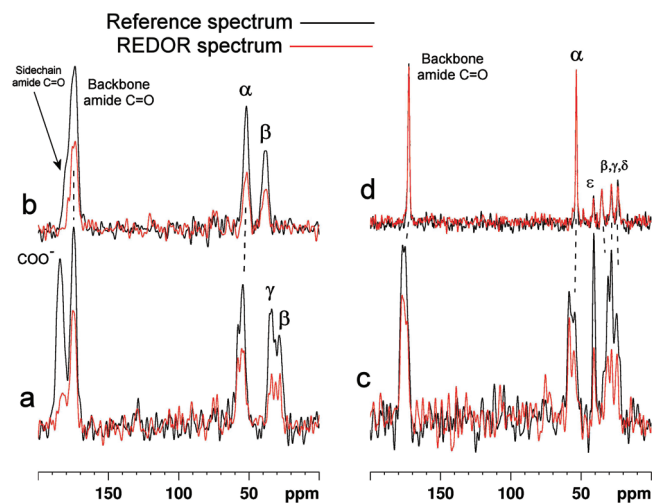


Figure 6. Typical REDOR (9.6 ms dephasing time) data from HAP composited with poly-L-glutamate (a), poly-L-asparagine (b), and poly-L-lysine (c), and from a mixture of particles of pure HAP and pure poly-L-lysine (d). Black and red traces have the same significance as in Figure 5.

Table 2. Relative REDOR Effects for HAP-Biopolymer Composites^a

| biopolymer-HAP composite | ¹³ C signal | | | | |
|--------------------------|-------------------------------------|-----------|-----------------|------------|-----------------|
| | carboxylate/ Amide Carbons | C-1 | ring carbons | NCH | CH ₃ |
| chondroitin sulfate | 0.62 | 0.68 | 0.60 | 0.56 | 0.63 |
| dermatan sulfate | 0.58 | 0.70 | 0.60 | 0.76 | 0.68 |
| hyaluronic acid | 0.8 | 0.71 | 0.56 | | 0.78 |
| dextran sulfate | | 0.73 | 0.69 | | |
| polygalacturonic acid | 0.76 | 0.83 | 0.80 | | |
| | C α | C β | C γ | C δ | C ϵ |
| polyGlu | 0.2 ^b , 0.6 ^c | 0.63 | 0.40 | | |
| polyAsn | 0.41 | 0.41 | 0.52 | | |
| polyLys | 0.78 | 0.60 | 0.42 | | 0.37 |

^a Integrated intensities of a given ¹³C signal were measured from reference spectra (black traces in Figures 5 and 6) and from REDOR spectra at 9.6 ms dephasing time (red traces in Figures 5 and 6), yielding S_0 and S_r , respectively. Fractional REDOR effects were calculated as S_r/S_0 . (A value of 1 would correspond to no REDOR effect). ^b Backbone amide ¹³C. ^c Side chain terminal carboxylate ¹³C.

corresponds to that of the majority of the ¹³C atoms in polysaccharide sugar rings, and a signal from carboxylate groups (ca. 180 ppm), there is a wealth of effects in protein signals as well, especially at longer REDOR dephasing times. Clearly interpretation of these effects in terms of participation of specific amino acid residues and, better still, specific proteins in the compositing process would provide extremely valuable insights into the mechanisms of biomineralization. As a first step toward producing a totally synthetic multicomponent composite which may be studied by these methods we coprecipitated HAP with equimolar (estimated on the basis of repeat residue effective molar mass) chondroitin sulfate, poly-L-glutamate and poly-L-lysine. REDOR results are shown in Figure 7a, accompanied for ease of comparison by those from an equivalent experiment on native bone (Panel b). Of course close similarities between bone and the simple multicomponent composite are not to be expected,

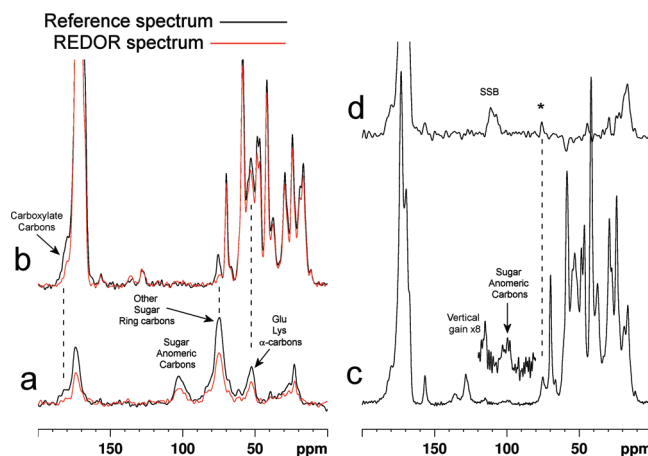


Figure 7. (a) A REDOR data set (9.6 ms dephasing time) from HAP cocomposited with equimolar (on the basis of repeat disaccharide or amino acid residue) amounts of chondroitin sulfate, poly-L-glutamate and poly-L-lysine. For clarity the results of a REDOR experiment on native bone are also shown (b), and some effects common to both materials are connected by vertical dashed lines. In bone in a standard CP acquisition the polysaccharide anomeric carbon signal at ca. 100 ppm is broad (c) and loses intensity rapidly to spin–spin relaxation processes; it is not observed in (b) at the long dephasing time used here. The results of 60 μ s dipolar dephasing at an MAS frequency of 6.25 kHz (d) show the contribution of a quaternary ¹³C signal (asterisked) to the bone 76 ppm signal. SSB—spinning sideband.

although the latter material does more closely resemble spectroscopically some of the organic deposits in apatitic uroliths. However, qualitatively at least, the artificial material recapitulates many of the REDOR features of real bone, in particular the pronounced effects to the 76 ppm and 180 ppm signals, and distinct effects to the poly amino acid α - and side chain carbons. Polysaccharide anomeric ¹³C signals are generally broad in bone samples (Panel c) and it is difficult to observe their participation in REDOR effects. In a step to more definitely assign the 76 ppm signal a dipolar dephasing experiment, which retains signal only from methyl and quaternary ¹³C atoms, was performed (Panel d). The result raises the possibility that in bone there is a contribution to the 76 ppm signal from quaternary ¹³C atoms which are not necessarily in polysaccharides.

Discussion

We have prepared HAP which we believe at the atomic scale mimics biogenic HAP in respect of mineral hydration, hydrogen phosphate substitutions, crystallinity, and nanoparticulate dimensions, under conditions of temperature and pH representative of biological conditions. Coprecipitation with a structurally diverse range of hydrophilic biopolymers produces composites with features which mimic many of the solid state NMR responses typical of native biological mineralized tissues.

Biopolymer–Mineral Contacts. Thus in most of the HAP materials coprecipitated with acidic polysaccharides considerable REDOR effects are observed (see Table 2). As in native biomineral there are distinctive effects to the high frequency signals between ca. 170 and 180 ppm corresponding to amide and carboxylate carbon atoms (when present in the structure), and to the intense peak at ca. 76 ppm corresponding to the majority of the

sugar ring carbon atoms. However the simplicity of the ^{13}C spectra relative to those of native biomineral allows us to observe and assign more effects to specific chemical functionalities. When present in the structure, the methyl group of *N*-acetylated sugars at ca. 25 ppm also undergoes a considerable REDOR effect, as does the aminated 2-carbon (ca. 50 ppm) in the same species and the envelope of overlapped 1-carbon (anomeric) signals at ca. 100 ppm. In native biomineral the two former signals are usually inextricably overlapped with protein (predominantly collagen) signals, and the latter generally too broad and weak to give useful information. An exception to the generally strong REDOR effects in the HAp – polysaccharide composites is provided by the polygalacturonic acid composite in which these effects are weaker. It may be significant that this is the only α -glycosidically linked polysaccharide studied, and that this polysaccharide forms strongly bound aggregates in the presence of Ca^{2+} ions. The rapid formation of aggregates could well prevent the formation of any mineral structure involving polygalacturonic acid-bound calcium.

In ideal cases such as those corresponding to isolated spin pairs in crystalline solids it is possible to analyze REDOR dephasing time dependences to extract accurate interatomic distances. Although we have quantified the REDOR effects we have not attempted such an analysis. This is because in a material of the type investigated here the REDOR effect on any ^{13}C atom almost certainly arises from several neighboring ^{31}P atoms. Even if the ^{31}P atoms were arranged in a well-defined crystal lattice structure mean interatomic distances extracted from REDOR data would still only be approximations. As it is, the material is only poorly ordered and assumptions about detailed mineral atomic locations cannot be made. As far as calculations are concerned the real situation is one of intractably complicated multiple spin interactions, and any quantification will only convey a false impression of precision.

Influence of Biopolymer Charge. Perhaps more interestingly, all the polysaccharides (except polygalacturonic acid as alluded to above) and poly aminoacids exhibit similarly close proximity to the mineral in the corresponding composites. Moreover, the tendency of each to composite is largely independent of the biopolymer charge. The importance of carboxylate¹³ and amide functionalities in the compositing process are testified by the strong REDORs observed to these carbons. Equally, the polycationic poly-L-lysine material also undergoes strong REDOR dephasing especially as regards its side chain β , γ , δ , and ϵ carbons. This argues that ideas regarding the mechanism of initiation of biomineralization should not focus entirely on recognition of calcium ions by anionic biopolymers.

It is hard to imagine that such a wide range of different molecular structures and conformations as represented by the selection of biopolymers used here can *all* act as templates for the same mineral structure. Another possibility is that the biopolymers here act as a collection area for the requisite ions in the mineral structure, perhaps

even allowing an amorphous calcium phosphate phase to form, from which the HAp structure then crystallizes. Many have postulated the formation of an amorphous phase prior to mineral crystal formation;³⁴ our own ^1H - ^{31}P HETCOR NMR results on the composites studied here and those on bone^{20,21} and other nanocrystalline hydroxyapatites³⁵ show the presence of disordered regions of the mineral containing strongly bound water and hydrogen phosphate. Moreover, these disordered regions have been shown to comprise a significant fraction of the phosphate in the mineral phase,³⁶ consistent with bone mineral comprising a poorly crystalline calcium phosphate phase within which nanocrystalline hydroxyapatite is embedded. Our results here would certainly support that concept.

What Role Could the Biopolymers Be Playing? The Drobny group has shown several cases³⁷ where proteins bind to preformed HAp via specific residues; such binding is the sort of process that is likely to inhibit the further growth of mineral crystals. Many others have postulated that various proteins can also act as templates for HAp crystal formation.^{2,7,8} Another possibility is that charged or polar biopolymers act to collect participating ions so as to allow the ordered formation of mineral crystals by control of local ion concentration. It must be noted that under the supersaturated reagent conditions employed here HAp precipitates even without biopolymer participation. A possibility that we cannot exclude is that the strong REDOR effects we observe are due to biopolymers becoming occluded in defects in the HAp lattice as it grows and propagates. Further work examining the influence of biopolymers on the precipitation of HAp from undersaturated solutions will be necessary to conclusively demonstrate their role.

It is nevertheless interesting to consider the wide variety of organic materials being used as scaffold materials for hard tissue replacement. These are variously based on molecules which occur naturally in the recipient tissue like collagen and polyanionic GAGs, convenient natural materials of diverse origins and composition including polycations like chitosan, and totally synthetic polymers which may be neutral or positively or negatively charged.³⁸ Of course many of these materials are chosen because they provide scaffolds favorable to the support and proliferation of osteogenic cells.³⁹ To the extent that scaffold organic materials may be influencing the osteoconductive process⁴⁰ our results suggest that part of this influence may take the form of modulating local ionic physical chemistry, consistent with the structural and electrostatic diversity tolerated among implant materials.

(34) Weiner, S. *Bone* **2006**, 39, 431.

(35) Jaeger, C.; Welzel, T.; Meyer-Zaika, W.; Eppler, M. *Magn. Reson. Chem.* **2006**, 44, 573.

(36) Schmidt-Rohr, K.; Rawal, A.; Fang, X. W. *J. Chem. Phys.* **2007**, 126, 054701.

(37) Stayton, P. S.; Drobny, G. P.; Shaw, W. J.; Long, J. R.; Gilbert, M. *Crit. Rev. Oral Biol. Med.* **2003**, 14, 370.

(38) Patel, M.; Fisher, J. P. *Pediatr. Res.* **2008**, 63, 497.

(39) Olivier, V.; Faucheux, N.; Hardouin, P. *Drug Discov. Today*. **2004**, 9, 803.

(40) Schwartz, Z.; Boyan, B. D. *J. Cell. Biochem.* **1994**, 56, 340.

Conclusions

We have synthesized biomimetic HAp composited with a variety of polysaccharides and poly amino acids. These materials recapitulate many of the atomic-level structural properties of natural apatitic biominerals, as revealed by NMR spectroscopy, but having a much simpler composition they will be much more amenable to detailed elucidation of intermolecular structural relationships. These approaches will be a useful complement to higher resolution structural studies on more complex native materials, and of biomineralization mechanisms. Finally, the NMR techniques described here, offering unequaled subnanometre level length scale evidence for intermolecular compositing of mineral and matrix biopolymers, may prove to

be the ultimate validation tool in in-life trials of osteointegration where ex vivo samples are available.

Acknowledgment. D. G. R. acknowledges the U. K. Biotechnology and Biological Sciences Research Council (B. B. S. R. C) for funding., and T. F. the Herchel Smith fund for a research fellowship. We thank Mr. Alan Dickerson (Department of Chemistry) for carbon, hydrogen and nitrogen elemental microanalysis.

Supporting Information Available: Plots of the dependence of the fractional REDOR effect S_i/S_0 on dephasing times of 4.8 and 9.6 ms for each of the composites are available online. This material is available free of charge via the Internet at <http://pubs.acs.org>.